Chapter Glossary

(ADCS)	Attitude Determination and Control System
(AutoNGC)	Autonomous Navigation, Guidance, and Control
(CoCom)	Coordinating Committee for Multilateral Export Controls
(COTS)	Commercial-off-the-Shelf
(DOF)	Degrees of Freedom
(DSAC)	Deep Space Atomic Clock
(DSN)	Deep Space Network
(EAR)	Export Administration Regulations
(FOGs)	Fiber Optic Gyros
(GNC)	Guidance, Navigation & Control
(GSO)	Geo-stationary Orbit
(USAF)	U.S. Air Force
(HCI)	Horizon Crossing Indicators
(IMUs)	Inertial Measurement Units
(JPL)	Jet Propulsion Laboratory
(LiDAR)	Light Detection and Ranging
(LMRST)	Low Mass Radio Science Transponder
(MarCO)	Mars Cube One
(PFF)	Precision Formation Flying
(PMSM)	Permanent-magnet Synchronous Motor
(PNT)	Position, Navigation, and Timing
(RPO)	Rendezvous and Proximity Operations
(SDST)	Small Deep Space Transponder
(SGP4)	Simplified General Perturbations 4
(SWaP)	Size, weight, and power
(TLE)	Two-Line Element
(TRL)	Technology Readiness Level
(USTP)	University SmallSat Technology Partnerships

5.0 Guidance, Navigation & Control

5.1 Introduction

The Guidance, Navigation & Control (GNC) subsystem includes the components used for position determination and the components used by the Attitude Determination and Control System (ADCS). In Earth orbit, onboard position determination can be provided by a Global Positioning System (GPS) receiver. Alternatively, ground-based radar tracking systems can also be used. If onboard knowledge is required, then these radar observations can be uploaded and paired with a suitable onboard orbit propagator. Commonly, the U.S. Air Force (USAF) publishes Two-Line Element sets (TLE) (1) which are paired with a Simplified General Perturbations 4 (SGP4) propagator (2). In deep space, position determination is performed using the Deep Space Network (DSN) and an onboard radio transponder (3). There are also technologies being developed that use optical detection of celestial bodies such as planets and X-ray pulsars to calculate position data (4).

Using SmallSats in cislunar space and beyond requires a slightly different approach than the GNC subsystem approach in low-Earth orbit. Use of the Earth's magnetic field, for example, is not possible in these missions, and alternate ADCS designs and methods must be carefully considered. Two communication relay CubeSats (Mars Cube One, MarCO) successfully demonstrated such interplanetary capability during the 2018 Insight mission to Mars (5). This interplanetary mission demonstrated both the capability of this class of spacecraft and the GNC fine pointing design for communication in deep space.

ADCS includes sensors to determine attitude and spin rate, such as star trackers, sun sensors, horizon sensors, magnetometers, and gyros. In addition, the ADCS is often used to control the vehicle during trajectory correction maneuvers and, using accelerometers, to terminate maneuvers when the desired velocity change has been achieved. Actuators are designed to change a spacecraft's attitude and to impart velocity change during trajectory correction maneuvers. Common spacecraft actuators include magnetic torquers, reaction wheels, and thrusters. There are many attitude determination and control architectures and algorithms suitable for use in small spacecraft (6).

Miniaturization of existing technologies is a continuing trend in small spacecraft GNC. While three-axis stabilized, GPS-equipped, 100 kg class spacecraft have been flown for decades, it has only been in the past few years that such technologies have become available for micro- and nano-class spacecraft. Table 5-1 summarizes the current state-of-the-art of performance for GNC subsystems in small spacecraft. Performance greatly depends on spacecraft size with a range of values for nano- to micro-class spacecraft.

The list of organizations/companies in this chapter is not all-encompassing and does not constitute an endorsement from NASA. There is no intention of mentioning certain companies and omitting others based on their technologies or relationship with NASA. The performance advertised may differ from actual performance since the information has not been independently verified by NASA subject matter experts and relies on information provided directly from the manufacturers or available public information. It should be noted that Technology Readiness Level (TRL) designations may vary with changes specific to the payload, mission requirements, reliability considerations, and/or the environment in which performance was demonstrated. Readers are highly encouraged to reach out to companies for further information regarding the performance and TRL of the described technology.

Table 5-1: State-of-the-Art GNC Subsystems		
Component	**Performance**	**TRL**
Reaction Wheels	0.00023 – 0.3 Nm peak torque, 0.0005 – 8 N m s storage	7-9
Magnetic Torquers	0.15 A m^2 – 15 A m^2	7-9
Star Trackers	8 arcsec pointing knowledge	7-9
Sun Sensors	0.1° accuracy	7-9
Earth Sensors	0.25° accuracy	7-9
Inertial Sensors	Gyros: 0.15° h^{-1} bias stability, 0.02° $h^{-1/2}$ ARW Accels: 3 µg bias stability, 0.02 (m s^{-1})/$h^{-1/2}$ VRW	7-9
GPS Receivers	1.5 m position accuracy	7-9
Integrated Units	0.002-5° pointing capability	7-9
Atomic Clocks	10 – 150 Frequency Range (MHz)	5-6
Deep Space Navigation	Bands: X, Ka, S, and UHF	7-9
Altimeters	~15 meters altitude, ~3 cm accuracy	7

5.2 State-of-the-Art – GNC Subsystems

5.2.1 Integrated Units

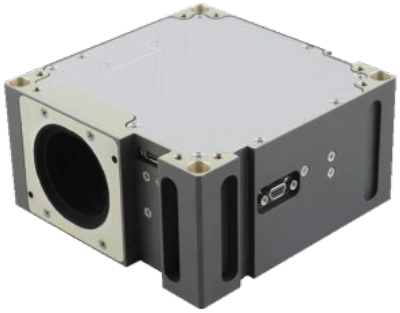

Figure 5.1: BCT XACT integrated ADCS unit. Credit: Blue Canyon Technologies.

Integrated units combine multiple different attitude and navigation components to provide a simple, single-component solution to a spacecraft's GNC requirements. Typical components included are reaction wheels, magnetometer, magnetic torquers, fine and/or coarse Sun sensors, GPS, and star trackers. The systems often include processors and software with attitude determination and control capabilities that enable common mission profiles such as Sun tracking, inertial pointing, and Earth target tracking. In addition, providers such as Blue Canyon Technologies (BCT) and CubeSpace can provide overall GNC design and simulation with their product to ensure that desired mission objectives can be met within the desired orbit environment and hardware constraints of the integrated unit and spacecraft bus. Using these integrated units can increase overall mission success, as the included ADCS software is also at a high TRL. BCTs' XACT (figure 5.1) flew on the NASA-led MarCO and ASTERIA missions, both of which were 6U platforms, and has also flown on 3U missions (MinXSS was deployed from NanoRacks in February 2016). Table 5-2 describes some of the integrated systems currently available that are associated with a TRL value of 7-9.

Table 5-2: Currently Available Integrated Systems							
Manufacturer	**Model**	**Mass (kg)**	**Actuators**	**Sensors**	**Processor**	**Pointing Accuracy**	**Ref**
AAC Clyde Space	iADCS-200	0.470	3 reaction wheels 3 magnetic torquers	1 star tracker 1 IMU, Optionally high precision magnetometer and sun sensors	Yes	<1°	(7)
	iADCS-400	1.7	3 reaction wheels 3 magnetorquers	1 star tracker, 1 IMU, Optionally high precision magnetometer and sun sensors	Yes	<1°	(8)
Arcsec	Arcus ADC	0.715	3 reaction wheels 3 magnetic torquers	1 star tracker 3 gyros 6 photodiodes 3 magnetometers	Yes	0.1°	(9)
Berlin Space Technologies	IADCS-100	0.4	3 reaction wheels 3 magnetic torquers	1 star tracker 3 gyros, 1 magnetometer, 1 accelerometer	Yes	<<1 deg	(10)
Blue Canyon Technologies	XACT-15	0.885	3 reaction wheels 3 magnetorquers	1 star tracker 3-axis magnetometer	Yes	0.003/0.007°	(11)
	XACT-50	1.230	3 reaction wheels 3 magnetorquers	1 star tracker 3-axis magnetometer	Yes	0.003/0.007°	(11)
	XACT-100	1.813	3 reaction wheels 3 magnetorquers	1 star tracker 3-axis magnetometer	Yes	0.003/0.007°	(11)
	Flexcore	†	3 – 4 reaction wheels 3 magnetorquers	2 star trackers 3-axis magnetometer	Yes	0.002°	(11)
CubeSpace Satellite Systems	CubeADCS	0.26*	3/4(Pyramid) x reaction wheels, 3 x Magnetorquers distributed or integrated with ADCS core (3U/6U only)	Up to 4 x FSS, 2 x EHS, 2 x STR, 2 x MGTM. All distributed	5Hz	~70 arcsec (3 sigma) †	(12)

*Mass may vary if actuators are integrated inside CubeADCS core.
†Configuration dependent.

5.2.2 Reaction Wheels

Miniaturized reaction wheels can provide small spacecraft with three-axis precision pointing capability. Reaction wheels provide torque and momentum storage along the wheel spin axis, which results in the spacecraft counter-rotating around the spacecraft center of mass due to conservation of angular momentum from the wheel spin direction. For example, the spacecraft deployment process typically results is some tipoff momentum that can be seen in induced spacecraft angular rates. This tipoff momentum can be stored in the reaction wheels, reducing the angular rate of the spacecraft to zero. Reaction wheels must be carefully selected based on several factors including the moment of inertia of the spacecraft, required momentum storage capacity, and mission slew rate requirements. Once a wheel reaches its maximum speed, it becomes saturated and can no longer provide a torque or store momentum in that axis/direction. To prevent this, reaction wheels need to be periodically desaturated using an actuator that provides an external torque, such as thrusters or magnetic torquers (13). By providing an external torque in an opposing direction, the reaction wheel compensates and spins down to keep the spacecraft at its target (14).

While one or two reaction wheels can be used for a momentum-biased spacecraft, a full three-axis controlled spacecraft requires at least three wheels mounted orthogonally. As reaction wheel failure is a common mode of failure in many missions, it is common to include three additional wheels as a hot backup (14). On smaller spacecraft where SWAP requirements prohibit redundant reaction wheels, a four-wheel configuration is often used to provide fault tolerance (15). The multiple reaction wheels are often assembled in a “skewed” or angled configuration such that there exists a cross-coupling of torques with two or more reaction wheels. While this reduces the torque performance in any single axis, it allows a redundant, albeit reduced, torque capability in more than one axis. The result is that should any single reaction wheel fail, one or more reaction wheels are available as a reduced-capability backup option.

Though reaction wheels are typically the primary choice for precision three-axis pointing, other important considerations must be made. For example, they can introduce major attitude disturbances through static and dynamic imbalances, which can generate undesired forces, torques, and moments. While placing reaction wheels near the center-of-gravity of spacecraft can help minimize the force/torque effects, other disturbances are location independent and careful design considerations must be made (14). Reaction wheels are typically not magnetically clean, whether it is in the electro-magnetic controller for spinning the wheels or ferrous materials being used in the wheel rotor itself, so consideration must be made when placing the wheels within the spacecraft bus. Wheels typically should be placed with sufficient separation from magnetometers or other sensitive instrumentation. As magnetic torquers are the primary method of preventing reaction wheel saturation for small spacecraft in Earth orbit, they require an accurate measurement of the Earth’s magnetic field to determine torquer commands, making wheel placement especially critical in the spacecraft bus design (17). Another consideration is how the reaction wheel is used in orbit and how precise pointing requirements are. Most reaction wheels have reduced performance around zero-crossings (transition between positive/negative speeds), so some missions choose to bias the momentum (i.e., wheels running at half maximum speed when at zero spacecraft angular rate) (18). This can provide finer control with less jitter, at the expense of reduced overall momentum capacity (effectively half).

Table 5-3 lists a selection of high-heritage miniature reaction wheels. Except for three units, all the reaction wheels listed have spaceflight heritage.

Table 5-3: High Heritage Miniature Reaction Wheels							
Manufacturer	**Model**	**Mass (kg)**	**Peak Power (W)**	**Peak Torque (Nm)**	**Momentum Capacity (Nms)**	**# Wheels**	**Radiation Tolerance (krad)**
AAC Clyde Space	RW210	0.48	0.8	0.0001	0.006	1	36
	RW400	0.375	15	0.008	0.050	1	36
	Trillian-1	1.5	24	47.1	1.2	1	--
Astrofein	RW1 Type A	≤ 0.025	< 0.375 + PWDE	23e-6	5.8e-4	1	/
	RW1 Type B	≤ 0.012	< 0.3 + PWDE	4e-6	1.0e-4	1	/
	RW25	≤ 0.2	< 2.8	0.002	0.03	1	/
	RW35	≤ 0.5	≤ 9	0.005	0.1	1	20
	RW90	≤ 0.9	≤ 16.5	0.015	0.35	1	20
	RW100	≤ 0.8	≤ 25	0.02	0.4	1	20
	RW150	≤ 1.3	≤ 42	0.03	1	1	20
	RWT150	≤ 1.5	≤ 120	0.1	1	1	20
	RW250	≤ 2.75	≤ 100	0.1	4	1	20
	RWT250	≤ 2.75	≤ 200	0.3	4	1	20
Berlin Space Technologies	RWA05	1.700	23.5	0.016	0.5	1	30
Blue Canyon Technologies	RWP015	0.130	1	0.004	0.015	1	--
	RWP050	0.240	1	0.007	0.050	1	--
	RWP100	0.330	1	0.007	0.100	1	--
	RWP500	0.750	6	0.025	0.500	1	--
	RW1	0.950	10	0.07	1.000	1	--
	RW4	3.200	10	0.250	4.000	1	--
	RW8	4.400	10	0.250	8.000	1	--
Comat	RW20	0.180	1	0.002	0.02	1	Up to 20Krad*
	RW40	0.230	1	0.004	0.04	1	Up to 20Krad*
	RW60	0.275	1	0.006	0.06	1	Up to 20Krad*
CubeSpace Satellite Systems	CubeWheel CW0017	0.06	0.85	0.23	0.0017	1/3/4(Pyramid)	24
	CubeWheel CW0057	0.115	2.7	2	0.0057	1/3/4(Pyramid)	24
	CubeWheel CW0162	0.144	7.2	7	0.0162	1/3/4(Pyramid)	24
CubeSpace Satellite Systems	CubeWheel CW0500	0.310	15	16	0.05	1/3/4(Pyramid)	24

Table 5-3: High Heritage Miniature Reaction Wheels							
Manufacturer	**Model**	**Mass (kg)**	**Peak Power (W)**	**Peak Torque (Nm)**	**Momentum Capacity (Nms)**	**# Wheels**	**Radiation Tolerance (krad)**
	CubeWheel CW1200	0.450*	32	20	0.12	1/3/4(Pyramid)	24
	CubeWheel CW2500	0.750*	33	27	0.25	1/3/4(Pyramid)	24
	CubeWheel CW5000	1.084	48	37	0.5	1/3/4(Pyramid)	24
	CubeWheel CW10K	2.1*	50	37	1	1/3/4(Pyramid)	24
	CubeWheel CW40K	2.2*	85	37	4	1/3/4(Pyramid)	24
GomSpace	NanoTorque GSW-600	0.940	0.3	0.0015	0.019	1	--
NanoAvionics	RWO	0.137	3.25	0.0032	0.020	1	20
	4RWO	0.665	6	0.0059	0.037	4	20
NewSpace Systems	NRWA-T6	<5	136	0.3	0.00783	1	20
	NRWA-T065	1.55	1.7	0.02	0.00094	1	10
	NRWA-T2	2.8	0.4	0.09	0.00163	1	10
Rocket Lab	RW-0.03	0.185	1.8	0.002	0.040	1	20
	RW-0.003	0.048	--	0.001	0.005	1	10
	RW-0.01	0.122	1.05	0.001	0.018	1	20
	RW3-0.06	0.235	23.4	0.020	0.180	1	20
	RW4-0.2	0.6	--	0.1	0.2	1	60
	RW4-0.4	0.77	--	0.1	0.4	1	60
	RW4-1.0	1.38	43	0.1	1	1	60
Vectronic Aerospace	VRW-A-1	1.90	110	0.090	6	1	20
	VRW-B-2	1.00	45	0.020	0.2	1	20
	VRW-C-1	2.3	45	0.020	1.2	1	20
	VRW-D-2	2	65	0.05	2.0	1	20
	VRW-D-6	3	110	0.09	6	1	20
VEOWARE	WHL-100	0.35		0.02	0.1	1	
	WHL-200	0.43		0.025	0.2	1	
	WHL-500	0.8		0.5	0.5	1	
	WHL-100	1.2		0.1	1	1	

*Printed Circuit Board (PCB) level

5.2.3 Magnetic Torquers

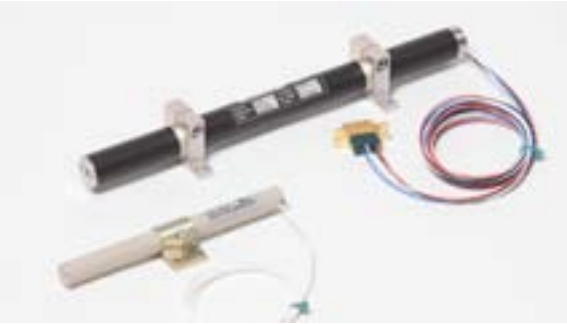

Figure 5.3: Magnetorquers for micro satellites. Credit: ZARM Technik.

Magnetic torquers provide control torques perpendicular to the local external magnetic field. They are divided into two categories, usually labeled as air coils or torquer bars/rods. Both operate by applying an electric field through a coiled conductor, generating a magnetic dipole through the center of the coil that loops around itself (14). This generated magnetic dipole interacts with the local external magnetic field, generating a torque perpendicular to the dipole and field. The strength of the dipole, and thereby the torque, is governed by the area of the coil and the number of turns in the coil. For torquer bars/rods, a ferrous core is added, which greatly amplifies the strength of the magnetic field without an increase in required power consumption. While these bars/rods typically provide volume and power savings, the ferrous material can hold a residual field even when the device is powered off, which can affect other sensitive instrumentation such as magnetometers. With air coils, however, residual magnetic fields dissipate very rapidly when powered off. Air coils typically need a larger coil radius and/or more windings with a higher power consumption requirement to provide an equivalent magnetic dipole as compared to torquer bars/rods. Many are custom designed specifically for the mission's spacecraft bus, such as being integrated into a components PCB inner layer. As such, not as many providers provide them as COTS components. Table 5-4 lists a selection of high heritage magnetic torquers and figure 5.3 illustrates some of ZARM Technik's product offerings.

As control torques can only be provided in the plane perpendicular to the local magnetic field and generated magnetic dipole, magnetic torquers alone cannot typically provide three-axis stabilization. A spacecraft will typically have three magnetic torquers mounted on orthogonal axes, and usually there is no need for redundant torquers as the electro-mechanical design provides internal redundancy (14). Some research shows that coarse three-axis pointing can be achieved, but this requires multiple orbits and sufficient orbit inclination to provide external magnetic field variability. Typically, magnetic torquers are often used to remove excess momentum from reaction wheels. As the torque generated from magnetic torquers acts externally to the spacecraft, the reaction wheels apply an internal counter torque to compensate and reduce their stored momentum. Magnetic torquers are also used on spinner missions, where they can slowly spin up the spacecraft by applying an external torque over time.

Use of magnetic torquers beyond low-Earth orbit and in interplanetary applications need to be carefully investigated since their successful operation is relying on a significant local external magnetic field. This magnetic field may or may not be available in the location and environment for that mission and additional control methods may be required.

Table 5-4: High Heritage Magnetic Torquers

Manufacturer	Model	Mass (kg)	Power (W)	Peak Dipole (A m^2)	# Axes	Radiation Tolerance (krad)
AAC Clyde Space	MTQ800	0.395	3	15	1	Unk
CubeSpace Satellite Systems	CubeTorquer CR0002	0.0165	0.49	0.2	1	24
	CubeTorquer CR0003	0.023	0.38	0.3	1	24

Table 5-4: High Heritage Magnetic Torquers						
Manufacturer	**Model**	**Mass (kg)**	**Power (W)**	**Peak Dipole (A m²)**	**# Axes**	**Radiation Tolerance (krad)**
CubeSpace Satellite Systems	CubeTorquer CR0004	0.023	0.63	0.4	1	24
	CubeTorquer CR0006	0.031	0.56	0.6	1	24
	CubeTorquer CR0008	0.028	0.56	0.8	1	24
	CubeTorquer CR0010	0.037	0.67	1	1	24
	CubeTorquer CR0012	0.045	0.68	1.2	1	24
	CubeTorquer CR0020	0.054	0.77	2	1	24
GomSpace	Nano Torque GST-600	-	-	0.31–0.34	3	-
	NanoTorque Z-axis Internal	0.106	-	0.139	1	-
ISISPACE	Magnetorquer Board	0.196	1.2	0.20	3	-
MEISEI	Magnetic Torque Actuator for Spacecraft	0.5	1	12	1	-
NanoAvionics	MTQ3X	0.205	0.4	0.30	3	-
	MTQ MP42	0.215	2.5	5	1	
NewSpace Systems	NCTR-M003	0.030	0.25	0.29	1	-
	NCTR-M012	0.053	0.8	1.19	1	-
	NCTR-M016	0.053	1.2	1.6	1	-
Rocket Lab	TQ-40	0.825	-	48.00	1	-
	TQ-15	0.400	-	19.00	1	-
ZARM Technik**	MT0.2-1	0.012-0.014	0.135-0.25	0.2	1	NA*
	MT0.5-1	0.009	0.275	0.5	1	NA*
	MT0.7-1-01	0.035	0.5	0.7	1	NA*
	MT1-1-01	0.065	0.23	1	1	NA*
	MT1.5-1-01	0.097	0.4	1.5	1	NA*
	MT2-1-02	0.1	0.5	2	1	NA*
	MT3-1-D22042701	0.15	0.7	3	1	NA*
	MT4-1	0.15	0.6	4	1	NA*
	MT5-1	0.19-0.3	0.73-0.75	5	1	NA*
	MT5-2	0.31	0.77	5	1	NA*
	MT6-2	0.25-0.3	0.48-1.1	6	1	NA*
	MT7-2	0.4	0.9	7	1	NA*
	MT10-1	0.35-0.4	0.53-0.8	10	1	NA*
	MT10-2	0.37-0.48	0.7-1	10	1	NA*
	MT15-1	0.4-0.55	1.0-1.55	15	1	NA*

* Only EEE parts are connector and wires. Magnetorquer is not sensitive to ionizing radiation.
** ZARM Technik: Over 200 models available with design to mass/power optimization.

5.2.4 Thrusters

Thrusters can generate forces and torques, providing spacecraft with both attitude and translational control capabilities (14). As they are not dependent on external fields or dynamics, they can be used in any orbit. However, they require some type of expendable fuel source, so the lifetime of the thruster can be limited. While not typically employed on SmallSats for attitude control, recent advances in the miniaturization of propulsion systems have resulted in some COTS availability. Thrusters have the advantage of providing large external torques to perform rapid maneuvers, quick reaction wheel desaturation, and spin stabilization. When used for attitude control, these systems can become more complex to prevent induced translational dynamics.

When these propulsion systems are used to provide orbit and/or translational control, attitude control remains necessary to control the direction of thrust. Even with a full three degree-of-freedom thruster system, depending on the thruster configuration and the center-of-gravity of the spacecraft, the thrusters can impart undesired torques that must be mitigated using attitude control systems such as reaction wheels or ACS thrusters.

One critical application of state-of-the-art thrusters is on proximity operation missions, an increasing area of focus for advanced mission concepts. Proximity operations require both high precision translational and attitude control that typically cannot be achieved with other actuators. Further discussion on this is provided in section 5.3.1. Translation and pointing accuracy are determined by minimum impulse bit and control authority by thruster force, with significant improvements recently being made in this field. An in-depth discussion on thrusters for attitude and translational control are described in Chapter 4: *In-Space Propulsion*.

5.2.5 Star Trackers

A star tracker can provide an accurate estimate of the absolute three-axis attitude by comparing a digital image to an onboard star catalog (15). Star trackers identify and track multiple stars and provide three-axis attitude up to several times a second (14). While simplistic in concept, star trackers are among the most expensive small spacecraft components with a significant variance in capabilities between manufactures. To operate, the sensor requires a clear field-of-view of a starfield such that an initial lost in space solution can be found. This initial acquisition depends on the FOV size, magnitude of the stars, and the star trackers internal processing capabilities. Factors such as spacecraft angular rate and external light sources and glare can corrupt and invalidate a solution. Missions dependent on accurate attitude information typically include an IMU propagated Kalman filter to maintain an attitude solution when the star tracker may lose track of an attitude solution. Mission design and star tracker integration into the spacecraft bus also requires careful geometry analysis to ensure that the FOV remains clear for critical mission operations. Missions with propulsion must also worry about contaminating the optics from thruster/exhaust plumes.

While all COTS star tracker suppliers can provide a full state attitude solution, it is their accuracy and capabilities in difficult situations that distinguishes the components and drastically increases their cost. Most modern star trackers can provide knowledge of the sensor's boresight to within a few arcseconds, with reduced knowledge about the roll-axis (14) when the spacecraft is inertially fixed. The accuracy is typically dependent on the optic's FOV, the sensor's resolution, and the processing power dictating the size of the star catalog. However, typically this accuracy can quickly degrade if the spacecraft has some angular rate. For example, cheaper star trackers might be able to track a solution at up to a 0.3 deg/s spacecraft angular rates, whereas more expensive options may track up to 3.0 deg/s. Other factors like stray light resilience, initial acquisition time, and precision also drive-up costs. State-of-the-art in this field revolves around improving the speed and accuracy of the sensors, as well as decreasing their size and mass. These advancements have allowed for new manufactures to enter the field with cheaper options,

allowing missions to get full 3-axis attitude information with a sensor that would otherwise be cost prohibitive. Table 5-5 lists some models suitable for use on small spacecraft. For example, Arcsec's Sagitta Star Tracker was launched on the SIMBA cubesat in 2020.

Table 5-5: Star Trackers Suitable for Small Spacecraft							
Manufacturer	**Model**	**Mass (kg)**	**Power (W)**	**FOV**	**Cross axis Accuracy (1 or 3s)**	**Twist Accuracy (1 or 3s)**	**Rad. Tol. (krad)**
Arcsec	Sagitta	0.275	1.4	25.4°	6	30	20
	Twinkle	0.04	0.6	10.4°	30	180	-
BAE Systems Inc, Space and Mission Systems	CT-2020	3.000	8	-	1.5"	1"	-
Berlin Space Technologies / AAC Clyde Space	ST200	0.040, 0.106*	0.65	22°	30"	200"	11
	ST400	0.250, 0.270*	0.75	15°	15"	150"	11
Blue Canyon Technologies	Standard NST	0.350	1.5	10° x 12°	6"	40"	-
	Extended NST	1.300	1.5	10° x 12°	6"	40"	-
Creare	UST	0.840	-	-	7"	15"	-
CubeSpace Satellite Systems	CubeStar	0.047	0.271	59.4°	0.02°	0.06°	24
Danish Technical University	MicroASC	0.425	1.9	-	2”	-	-
Jena-Optronik	ASTRO CL	0.305	<1.0	25° full cone	6"	48"	50
	ASTRO APS	~2	<6 (<12 w/ TEC)	20° full cone	3"	24"	100
	ASTRO APS3	1.8	<6 (<8 w/ TEC)	20° full cone	2.4"	21"	100
Leonardo	Spacestar	1.600	6	20° x 20°	7.7"	10.6"	-
NanoAvionics	ST-1	0.108	1.2	21° full-cone	8"	50"	20
Redwire Space	Star Tracker	0.475	2.5	14x19	10/27"	51"	75
Rocket Lab	ST-16RT2	0.185	1	8° half-cone	5"	55"	-
Sodern	Auriga	0.225	0.8	30°	10"	70"	35
	Hydra	1.4	0.7	22°	3"	30"	50
	Horus	1.6	9.5	23,6°	3"	30"	50
Solar MEMS Technologies	STNS	0.14	1	12°	40"	70"	20
Space Micro	MIST	0.520	3	14.5°	15"	105"	30
	µSTAR-100M	1.800	5	-	15"	105"	100
	µSTAR-200M	2.100	8-10	-	15"	105"	100
	µSTAR-200H	2.700	10	-	3"	21"	100
	µSTAR-400M	3.300	18	-	15"	105"	100
Terma	T1	0.637 OH	0.8 OH*, 2.5	20° circular	3.0"	21"	55†
	T3	0.45 (DPU) 0.330	2	20° circular	3.2"	22"	35
Vectronic Aerospace	VST-41MN	0.7 - 0.9	2.5	14° x 14°	27"	183"	20
	VST-68M	0.470	3	14° x 14°	7.5"	45"	20

*Mass includes Baffle.
†SEE Immune

5.2.6 Magnetometers

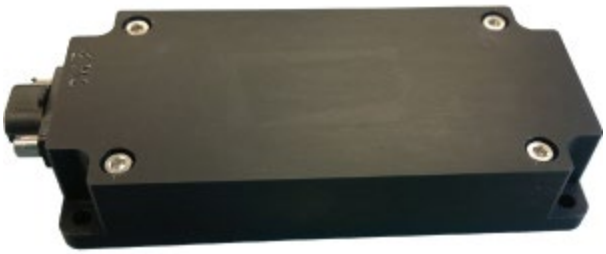

Figure 5.4: NSS Magnetometer. Credit: NewSpace Systems.

Magnetometers provide a measurement of the local magnetic field, which can be used to provide a real-time estimate of 2-axis attitude information (20). This requires that a well modeled magnetic field model is available to reference the measured magnetic field (14). With a time-history of magnetometer data, algorithms exist (such as Kalman filters) that can provide full state attitude and rate knowledge from magnetometer only measurements. Using other sources of unit vector measurements (i.e., Sun sensor for Sun vector knowledge) can provide real-time 3-axis attitude information by using algorithms such as TRIAD and QUEST. In addition to attitude information, knowing the local magnetic field is required to determine the necessary dipole for magnetic torquers to produce a desired external torque on the spacecraft.

As a magnetometer cannot differentiate between different sources of magnetic fields, placement on the spacecraft bus must be carefully considered. Sources like reaction wheels and magnetic torquer rods can change the local magnetic field, as well as other sources of electromagnetic fields like power systems, cabling harnesses, and even solar cells (14). Spacecraft with critical magnetic field measurement requirements may choose to place the magnetometer on a boom extending from the spacecraft, as magnetic dipole falls off at the cubed reciprocal of distance. In addition to careful spacecraft placement, experience has shown that magnetometers may require on-orbit recalibration, which requires orbit position and preferably attitude data. Table 5-6 provides a summary of some three-axis magnetometers available for small spacecraft, one of which is illustrated in figure 5.4.

Table 5-6: Three-axis Magnetometers for Small Spacecraft

Manufacturer	Model	Mass (kg)	Power (W)	Resolution (nT)	Orthogonality	Rad Tolerance (krad)
AAC Clyde Space	MM200	0.012	0.01	1.18	-	30
	MAG-3	0.100	Voltage Dependent	-	1°	10
CubeSpace Satellite Systems	CubeMag Deployable	0.016	0.23	13	0.6	24
	CubeMag Compact	0.006	0.23	25	0.6	24
GomSpace	NanoSense M315	0.008	-	-	-	-
NewSpace Systems	NMRM-Bn25o485	0.085	0.75	8	1°	10
MEISEI	3-Axis Magnetometer for Small Satellite	0.220	1.5	-	1°	-
ZARM Technik	Analogue High-Rel Fluxgate Magnetometer FGM-A-75	0.33	0.75 W	±75000	1°	50
	Digital AMR Magnetometer AMR-D-100-EFRS485	0.18	0.3 W	±100000	1°	-

5.2.7 Sun Sensors

Figure 5.5: Redwire coarse Sun sensor detector (cosine type). Credit: Redwire Space.

Sun sensors are used to estimate the direction of the Sun in a spacecraft body frame. Sun direction estimates can be used for attitude estimation, though to obtain a three-axis attitude estimate at least one additional independent source of attitude information is required (e.g., the Earth nadir vector or the direction to a star). Because the Sun is easily identifiable and extremely bright, Sun sensors are often used for fault detection and recovery. However, care must be taken to ensure the Moon or Earth's albedo is not inadvertently perturbing the measurement. Even glint off nearby spacecraft components can corrupt measurements for some types of Sun sensors (14). One method to limit albedo effects is to exclude measurements below a certain brightness threshold (albedo is typically measured as some fraction of solar maximum), but care must be taken with this method as it may limit the effective field-of-view of the sensor (cutoff threshold corresponds to the solar angle yielding the same cosine loss). Commercial examples of small spacecraft Sun sensors are described in table 5-7.

There are several types of Sun sensors which operate on different principles.

Cosine detectors are photocells. Their output is the current generated by the cell, which is (roughly) proportional to the cosine of the angle between the sensor boresight and the Sun. Typically several cosine detectors (pointing in different directions) are used on a spacecraft for full sky coverage. These sensors are the most susceptible to albedo effects. Cosine detectors (e.g., figure 5.5) are inexpensive, low-mass, simple and reliable devices, but their accuracy is typically limited to a few degrees, and they do require analog-to-digital converters.

Quadrant detectors. Quadrant sun sensors typically operate by shining sunlight through a square window onto a 2 x 2 array of photodiodes. The current generated by each photodiode is a function of the direction of the Sun relative to the sensor boresight. The measured currents from all four cells are then combined mathematically to produce the angles to the Sun. While more accurate than Cosine detectors, they have a similar sensitivity to albedo effects.

Digital Sun Sensor. The Sun illuminates a narrow slit with a number of photodiodes located behind a geometric coded bit mask. Depending on the angle to the Sun, the photodiodes will be illuminated as per the geometric pattern resulting in correspondingly different photocurrents which are then amplified and thresholded against an average value. Given the known slit geometries, this digital bit output can then be converted to a sun angle.

Sun Camera. Some Sun sensors are built as a small camera imaging the Sun. Since the Sun is so bright, the optics include elements to decrease the thoughput. A computer will identify the image of the Sun and calculate the centroid. Sun sensors can be made very accurate this way and typically have built in albedo rejection. Sometimes, multiple apertures are included to increase accuracy.

Table 5-7: Small Spacecraft Sun Sensors										
Manufacturer	**Model**	**Sensor Type**	**Mass (kg)**	**Peak Power (W)**	**Analog or Digital**	**FOV**	**Accuracy (3s)**	**# Measurement Angles**	**Radiation Tolerance (krad)**	**TRL**
AAC Clyde Space	SS200	-	0.003	0.04	Digital	110°	<1°	-	>36	7-9
Berlin Space Technologies	FSSA-110	Fine Sun Sensor	With 3x sensor: 0.102	0.185	Analog	114°	5°	?	>20	7-9
Bradford Space	CoSS	Cosine	0.024	0	Analog	160° full cone	3°	1	40000	7-9
	CoSS-R	Cosine	0.015	0	Analog	180° full cone	3°	1	120000	7-9
	CSS	Cosine	0.215	0	Analog	180°x180°	1.5°	2	70000	7-9
	FSS	Quadrant	0.375	0.25	Analog	128° x 128°	0.3°	2	100	7-9
	Mini-FSS	Quadrant	0.050	0	Analog	128° x 128°	0.2°	2	20000	7-9
CubeSpace Satellite Systems	CubeSense	Camera	0.015	0.174	Digital	0.2°	2	24	CubeSense	7-9
GomSpace	NanoSense FSS	Quadrant	0.002	-	Digital	45°, 60°	±0.5°, ±2°	2	-	-
Lens R&D	BiSon64-ET	Quadrant	0.023	0	Analog	±58° per axis	0.5°	2	9200	7-9
	BiSon64-ET-B	Quadrant	0.033	0	Analog	±58° per axis	0.5°	2	9200	7-9
	MAUS	Quadrant	0.014	0	Analog	±57° per axis	0.5°	2	9200	7-9
Needronix	Eagle	Fine Sun Sensor (±55°)	0.003	<0.007	Digital	110°	< ±0.15°	2 plus Irradiation and Gyro	>20	7-9
	Eagle Plus	Fine Sun Sensor (±55°)	0.005	<0.015	Digital	110°	< ±0.1°	2 plus Irradiation and Gyro	>20	5-6
	Eagle Point	Fine Sun Pointing (±5.5°)	0.006	<0.015	Digital	11°	< ±0.01°	2 plus Irradiation and Gyro	>20	5-6

Table 5-7: Small Spacecraft Sun Sensors										
Manufacturer	**Model**	**Sensor Type**	**Mass (kg)**	**Peak Power (W)**	**Analog or Digital**	**FOV**	**Accuracy (3s)**	**# Measurement Angles**	**Radiation Tolerance (krad)**	**TRL**
	Swan	Coarse Sun Sensor Pyramid	0.070	0	Analog	170° (~ 2π Steradian)	< ±1° (Region I.)	2	>1000	5-6
NewSpace Systems	NFSS-411	-	0.035	0.150	Digital	140°	0.1°	--	20	7-9
	NCSS-SA05	-	0.005	0.05	Analog	114°	0.5°	--	-	7-9
Redwire Space	Coarse Analog Sun Sensor	Coarse Analog Sun Sensor	0.045	0	Analog	±40°	±1°	1	>100	7-9
	Coarse Sun Sensor (Cosine Type)	Coarse Sun Sensor (Cosine Type)	0.010	0	Analog	~ Cosine, Conical Symmetry	±2° to ±5°	Configuration dependent	>100	7-9
	Coarse Sun Sensor Pyramid	Coarse Sun Sensor Pyramid	0.13	0	Analog	2π steradian+	±1° to ±3°	2	>100	7-9
	Digital Sun Sensor (±32°)	Digital Sun Sensor (±32°)	Sensor 0.3 kg Electronics ~1	1	Digital	±32° x ±32° (each sensor)	±0.125°	2	100	7-9
	Digital Sun Sensor (±64°)	Digital Sun Sensor (±64°)	Sensor0.25 Electronics 0.29 - 1.1	0.5	Digital	128° X 128° (each sensor) Note: 4π steradians achieved with 5 sensors	±0.25°	2	100	7-9

Table 5-7: Small Spacecraft Sun Sensors										
Manufacturer	**Model**	**Sensor Type**	**Mass (kg)**	**Peak Power (W)**	**Analog or Digital**	**FOV**	**Accuracy (3s)**	**# Measurement Angles**	**Radiation Tolerance (krad)**	**TRL**
	Fine Pointing Sun Sensor	Fine Pointing Sun Sensor	Sensor .95 Electronics 1.08	< 3	Digital	±4.25° x ±4.25° (Typical)	Better than ±0.01°	2	100	7-9
	Fine Spinning Sun Sensor (±64°)	Fine Spinning Sun Sensor (±64°)	Sensor 0.109 Electronics 0.475 – 0.725	0.5	Analog and Digital	±64° Fan Shaped (each sensor)	±0.1°	1 plus Sun Pulse	100	7-9
	Micro Sun Sensor	Micro Sun Sensor	< 0.002	< 0.02	Analog	± 85° Minimum	±5°	2	Approx. 10	5-6
	Miniature Spinning Sun Sensor (±87.5°)	Miniature Spinning Sun Sensor (±87.5°)	< 0.25	0.5	Digital	±87.5° (From normal to spin axis)	±0.1°	1 plus Sun Pulse	100	7-9
	Fine Sun Sensor (±50°)	Fine Sun Sensor (±50°)	-	-	Digital	100 X 100 Each Sensor	±0.01° TO ±0.05°	2	100, 150, or 300	7-9
Solar MEMS Technologies	nanoSSOC-A60	Orthogonal	0.004	0.007	Analog	±60° per axis	0.5°	2	100	7-9
	nanoSSOC-D60	Orthogonal	0.007	0.076	Digital	±60° per axis	0.5°	2	30	7-9
	SSOC-A60	Orthogonal	0.025	0.01	Analog	±60° per axis	0.5°	2	100	7-9
	SSOC-D60	Orthogonal	0.035	0.315	Digital	±60° per axis	0.5°	2	30	7-9
	ACSS	Quadrant & Redundant	0.035	0.072	Analog	±60° per axis	0.5°	2	200	7-9
Space Micro	CSS-01, CSS-02	Cosine	0.010	0	Analog	120° full cone	5°	1	100	7-9
	MSS-01	Quadrant	0.036	0	Analog	48° full cone	1°	2	100	7-9

5.2.8 Horizon Sensors

Horizon sensors can be simple infrared horizon crossing indicators (HCI), or more advanced thermopile sensors that can detect temperature differences between the poles and equator. The sensors are typically either static or scanning, but by characterizing horizon crossings over a series of measurements, the sensors can provide an accurate nadir vector, which can then be used for attitude determination and/or attitude control guidance (14). For terrestrial applications, these sensors are referred to as Earth Sensors, but can be used for other planets. Examples of such technologies are described in table 5-8 and illustrated in figure 5.6.

Figure 5.6: MAI-SES. Credit: Redwire Space.

In addition to the commercially-available sensors listed in table 5-8, there has been some recent academic interest in horizon sensors for CubeSats with promising results (4)(21)(22).

Table 5-8: Commercially Available Horizon Sensors

Manufacturer	Model	Sensor Type	Mass (kg)	Peak Power (W)	Analog or Digital	Accuracy	# Measurement Angles	Rad Tolerance (krad)
CubeSpace Satellite Systems	CubeSense Earth	Infrared camera	0.018	0.28	Digital	1°	-	24
Servo	Mini Digital HCI	Pyroelectric	0.050	Voltage Dependent	Digital	0.75°	Unk	Unk
	RH 310 HCI	Pyroelectric	1.5	1	Unk	0.015°	Unk	20
Solar MEMS Technologies	HSNS	Infrared	0.120	0.150	Digital	1°	2	30

5.2.9 Inertial Sensing

Inertial sensors include gyroscopes for measuring angular change and accelerometers for measuring velocity change. They are packaged in different ways that range from single-axis devices (i.e., a single gyroscope or accelerometer), to packages which include 3 orthogonal axes of gyroscopes (Inertial Reference Unit (IRU)) to units containing 3 orthogonal gyros and 3 orthogonal accelerometers (Inertial Measurement Unit (IMU)). These sensors are frequently used to propagate the vehicle state between measurement updates of a non-inertial sensor. For example, star trackers typically provide attitude updates at a few Hertz. If the control system requires accurate knowledge between star tracker updates, then an IMU may be used for attitude propagation between star tracker updates.

Gyroscope technologies typically used in modern small spacecraft are fiber optic gyros (FOGs) and MEMS gyros, with FOGs usually offering superior performance at a mass and cost penalty (24). While MEMs are smaller and can provide sufficient performance, they are more susceptible to radiation and single event upsets, with radiation hardened models only recently becoming

available (14). Other gyroscope types exist (e.g., resonator gyros, ring laser gyros), but these are not common in the SmallSat/CubeSat world due to size, weight, and power (SWaP) and cost considerations.

Gyro behavior is a complex topic (25) and gyro performance is typically characterized by a multitude of parameters. Table 5-9 only includes bias stability and angle random walk for gyros, and bias stability and velocity random walk for accelerometers, as these are often the driving performance parameters. That said, when selecting inertial sensors, it is important to consider other factors such as dynamic range, output resolution, bias, sample rate, etc. Factors like turn-on bias and bias drift require onboard estimation of the bias so that the sensor can be used in attitude determination and control systems.

Table 5-9: Gyros Available for Small Spacecraft													
Manufacturer	**Model**	**Sensor Type**	**Technology**	**Mass (kg)**	**Power (W)**	**Gyros**				**Accelerometers**			
							Bias Stability		**ARW**		**Bias Stability**		**VRW**
						# Axes	**(°/hr)**	**stat**	**(°/rt(hr))**	**# Axes**	**(µg)**	**stat**	**(m/sec)/rt(hr)**
Emcore	QRS11	Gyro	MEMS	≤0.06	0.8	1	6	Typical	-	-	-	-	-
	QRS28	Gyro	MEMS	≤0.025	0.5	2	-	-	-	-	-	-	-
Honeywell	MIMU	IMU	RLG	4	34	3	0.05	-	0.01	-	100	-	-
	HG1700	IMU	RLG	0.9	5.000	3	1.000	1σ	0.125	3	1000	1σ	0.65
	HG4934SRS (PN: 68904934-BA60)	IRU	MEMS	0.145	<5.500 peak	3	< 3.0	3s	<0.20 max	None, IRU only	None, IRU only	None, IRU only	None, IRU only
L3	CIRUS	Gyros	FOG	15.400	40.000	3	0.000	1σ	0.100	0	-	-	-
NewSpace Systems	NSGY-001	IRU	Image-based rotation estimate	0.055	0.200	3	-		-	0	-	-	-
Northrop Grumman	LN-200S	IMU	FOG, SiAc	0.748	12	3	1.000	1σ	0.070	3	300	1σ	-
NovAtel	OEM-IMU-STIM300	IMU	MEMS	0.055	1.50	3	0.500	--	0.150	3	50	-	0.060
Safran	STIM202	IRU	MEMS	0.055	1.500	3	0.400	--	0.170	0	-	-	-
	STIM210	IRU	MEMS	0.052	1.500	3	0.300	--	0.150	0	-	-	-
	STIM300	IMU	MEMS	0.055	2.000	3	0.300	--	0.150	3	50	--	0.07

Table 5-9: Gyros Available for Small Spacecraft													
Manufacturer	Model	Sensor Type	Technology	Mass (kg)	Power (W)	Gyros				Accelerometers			
							Bias Stability		ARW		Bias Stability		VRW
						# Axes	(°/hr)	stat	(°/rt(hr))	# Axes	(µg)	stat	(m/sec)/rt(hr)
	STIM318	IMU	MEMS	0.057	2.500	3	0.300	--	0.150	3	3	--	0.015
	STIM320	IMU	MEMS	0.057	2.500	3	0.300	--	0.100	3	3	--	0.015
	STIM277H	IRU	MEMS	0.052	1.500	3	0.300	--	0.150	0	-	--	-
	STIM377H	IMU	MEMS	0.055	2.000	3	0.300	--	0.150	3	50	--	0.07
Silicon Sensing Systems	CRH03	Gyro	MEMS	0.42	0.2W	1	CRH03-010 – 0.03 CRH03-025 – 0.04 CRH03-100 – 0.04 CRH03-200 – 0.05 CRH03-400 – 0.1		CRH03-010 – 0.005 CRH03-025 – 0.006 CRH03-100 – 0.006 CRH03-200 – 0.008 CRH03-400 – 0.010	0	-	-	-
	CRH03 (OEM)	Gyro	MEMS	0.18	0.2W	1	CRH03-010 – 0.03 CRH03-025 – 0.04 CRH03-100 – 0.04 CRH03-200 – 0.05		CRH03-010 – 0.005 CRH03-025 – 0.006 CRH03-100 – 0.006	0	-	-	-

Table 5-9: Gyros Available for Small Spacecraft													
Manufacturer	**Model**	**Sensor Type**	**Technology**	**Mass (kg)**	**Power (W)**	**Gyros**				**Accelerometers**			
							Bias Stability		**ARW**		**Bias Stability**		**VRW**
						# Axes	**(°/hr)**	**stat**	**(°/rt(hr))**	**# Axes**	**(µg)**	**stat**	**(m/sec)/rt(hr)**
							CRH03-400 – 0.1		CRH03-200 – 0.008 CRH03-400 – 0.010				
	RPU30	Gyro	MEMS	1.35	<0.8W	3	0.06		0.006	0	-	-	-
	DMU41	9 DoF IMU	MEMS	<2	<1.5W	3	0.1		0.015	3	15	-	0.05
	CAS	Acc	MEMS	0.004	-	0	-		-	2	CAS2X1S - 7.5 CAS2X2S - 7.5 CAS2X3S - 7.5 CAS2X4S - 25 CAS2X5S - 75		CAS2X1S - TBC CAS2X2S - TBC CAS2X3S - TBC CAS2X4S - TBC CAS2X5S - TBC
VectorNav	VN-100*	IMU + magnetometers +barometer	MEMS	0.015	0.220	3	10.000	max	0.210	3	40	max	0.082
	VN-110*	IMU + magnetometers	MEMS	0.125	2.500	3	1.000	max	0.0833	3	10	max	0.024

*Small form-factor versions of these products available.
-- Represents unknown data

5.2.10 GPS Receivers

For low-Earth orbit spacecraft, GPS receivers are now the primary method for performing orbit determination, replacing ground-based tracking methods. Onboard GPS receivers are now considered a mature technology for small spacecraft, and some examples are described in Table 5-10. There are also next-generation chip-size COTS GPS solutions, for example the NovaTel OEM 719 board has replaced the ubiquitous OEMV1.

By measuring the time between receiving signals between multiple GPS spacecraft, the GPS receiver can determine its position to a high degree of accuracy (14). A minimum of four spacecraft must be visible to the GPS receiver, where three provide position data and a fourth provides timing to correct the GPS receivers clock bias. With multiple GPS antennas, a spacecraft's GPS receiver can even be used for attitude determination by using phase differences in GPS signals, though the accuracy of this method is limited and prone to error sources. GPS accuracy is limited by propagation variance through the exosphere and the underlying precision of the civilian use C/A code (26). GPS units are controlled under the Export Administration Regulations (EAR) and must be licensed to remove Coordinating Committee for Multilateral Export Control (COCOM) limits (27).

Although the usability of GPS is limited to LEO missions, past experiments have demonstrated the ability of using a weak GPS signal at GSO, and potentially soon to cislunar distances (29)(28). Development and testing in this fast-growing area of research and development may soon make onboard GPS receivers more commonly available.

Table 5-10: GPS Receivers for Small Spacecraft

Manufacturer	Model	Mass (kg)	Power (W)	Accuracy (m)	Radiation Tolerance (krad)
AAC Clyde Space	GNSS-701	0.16	--	<5	10
APL	Frontier Radio Lite	0.4	1.4	15	20
Aerospacelab	GNSS-VSP	0.394	2.4	1.5 (RMS)	*
General Dynamics	Explorer	1.2	8	15	-
	Viceroy-4	1.1	8	15	-
GomSpace	0.285	3	< 10	<20	0.285
NovaTel	OEM 719	0.031	0.9	-	*
SkyFox Labs	piNAV-NG	0.024	0.124	10	30
Spacemanic	Celeste_gnss_rx	0.025	~0.1	1.5	40
Surrey Satellite Technology	SGR-Ligo	0.09	0.5	5	5

*Heavy ions (61 MeV) No destructive event Except OEM719 receiver which is protected by smart current limit

5.2.11 Deep Space Navigation

Figure 5.7: General Dynamics SDST. Credit: General Dynamics.

In deep space, navigation is performed using radio transponders in conjunction with the Deep Space Network (DSN). As of 2020, the only deep space transponder with flight heritage suitable for small spacecraft was the JPL-designed and General Dynamics-manufactured Small Deep Space Transponder (SDST). JPL has also designed IRIS V2, which is a deep space transponder that is more suitable for the CubeSat form factor. Table 5-11 details these two radios, and the SDST is illustrated in figure 5.7. IRIS V2, derived from the Low Mass Radio Science Transponder (LMRST), has flown on the MarCO CubeSats in 2018, LICIACube that performed an asteroid flyby in September 2022, 12U lunar CAPSTONE spacecraft that entered a lunar orbit November 13, 2022, and was on six Artemis 1 secondary CubeSat payloads (Lunar Flashlight, LunaH-Map, ArgoMoon, CubeSat for Solar Particles, Biosentinel, and NEA Scout). It is also scheduled to fly on INSPIRE (30).

Table 5-11: Deep Space Transponders for Small Spacecraft

Manufacturer	Model	Mass (kg)	Rx Power (W)	Bands	Radiation Tolerance (krad)
General Dynamics	SDST	3.2	12.5	X, Ka	50
Space Dynamics Laboratory	IRIS V2.1	1.1	10.3	X, Ka, S, or UHF	25
	Iris Radio V3	0.8	10	Simultaneous Multi-band: X, Ka, S	25

5.2.12 Atomic Clocks

Atomic clocks have been used on larger spacecraft in low-Earth orbit for several years now, however integrating them on small spacecraft is relatively new. Table 5-12 provides examples of commercially available atomic clocks and oscillators for SmallSats. The conventional method for spacecraft navigation is a two-way tracking system of ground-based antennas and atomic clocks. The time difference from a ground station sending a signal and the spacecraft receiving the response can be used to determine the spacecraft's location, velocity, and (using multiple signals) the flight path. This is not a very efficient process, as the spacecraft must wait for navigation commands from the ground station instead of making real-time decisions, and the ground station can only track one spacecraft at a time, as it must wait for the spacecraft to return a signal (31). In deep space navigation, the distances are much greater from the ground station to spacecraft, and the accuracy of the radio signals needs to be measured within a few nanoseconds.

More small spacecraft designers are developing their own version of atomic clocks and oscillators that are stable and properly synchronized for use in space. They are designed to fit small spacecraft, for missions that are power- and volume-limited or require multiple radios.

Table 5-12: Atomic Clocks and Oscillators for Small Spacecraft							
Manufacturer	**Model**	**Dimensions (mm)**	**Mass (kg)**	**Power (W)**	**Frequency Range (MHz)**	**Rad Tolerance (krad)**	**TRL**
AccuBeat	Ultra Stable Oscillator	131 x 120 x 105	2	6.5	57.51852	50	7-9
Bliley Technologies	Iris Series 1"x1" OCXO for LEO	19 x 11 x 19	0.016	1.5	10 -100	39	7-9
	Aether Series TCVCXO for LEO	21 x 14 x 8	-	0.056	10 - 150	37	-
Microsemi	Space Chip Scale Atomic Clock (CSAC)	41 x 36 x 12	0.035	0.12	10	20	5-6
Safran Timing Technologies SA	MO	44 x 54 x 57	0.22	3.5 Nom 5.5 Max	10	100	-
	Space Qualified mRO-50	51 x 51 x 20	0.080	0.4 Nom	10	25 Min	-
	miniRAFS	108 x 53 x 68	0.45	< 12 Max	60 and 10	--	-
	LNMO	50 x 50 x 30	0.1	1.5 Nom 2.5 Max	5 – 40	100	-

- Represents unknown data

5.2.13 LiDAR

Light Detection and Ranging (LiDAR) is new type of sensor that is emerging. The technology has matured in terrestrial applications (such as automotive applications) over the last decade and is used in larger spacecraft that are capable of proximity operations, like Orion. This sensor type has applications for small spacecraft altimetry and relative navigation (e.g., a Mars helicopter, rendezvous and docking, and formation flying). Table 5-13 lists examples of flown LiDARs.

Table 5-13: Lidar for Small Spacecraft					
Manufacturer	**Model**	**Mass (kg)**	**Power (W)**	**Max Range (m)**	**Radiation Tolerance (krad)**
ASC	GSFL-4K (3D)	3	30	>1 km in altimeter mode	-
Garmin	Lidar Lite V3	0.022	0.7	40	-

- Represents unknown data

5.3 On the Horizon

In general, technological progress in guidance, navigation, and control is advancing quickly in automotive research areas but is lagging slightly in the aerospace industry. Given the high maturity of existing GNC components, future developments in GNC are mostly focused on incremental or evolutionary improvements, such as decreases in mass and power, and increases in longevity and/or accuracy. This is especially true for GNC components designed for deep space missions that have only very recently been considered for small spacecraft. However, in a collaborative effort between the Swiss Federal Institute of Technology and Celeroton, there is progress being made on a high-speed magnetically levitated reaction wheel for small satellites (figure 5.8). The idea is to eliminate mechanical wear and stiction by using magnetic bearings rather than ball bearings. The reaction wheel implements a dual hetero/homopolar, slotless, self-bearing, permanent-magnet synchronous motor (PMSM). The fully active, Lorentz-type magnetic bearing consists of a heteropolar self-bearing motor that applies motor torque and radial forces on one side of the rotor's axis, and a homopolar machine that exerts axial and radial forces to allow active control of all six degrees of freedom. It can store 0.01 Nm of momentum at a maximum of 30,000 rpm, applying a maximum torque of 0.01 Nm (32).

Figure 5.8: High-speed magnetically levitated reaction wheel. Credit: Celeroton AG.

Several projects funded via NASA's Small Spacecraft Technology (SST) program through the University SmallSat Technology Partnerships (USTP) initiative have begun advancing GNC systems. Listed below in table 5-14 are projects that focused on GNC advancement, and further information can be found at the USTP website:

https://www.nasa.gov/smallspacecraft/university-smallsat-technology-partnership-initiative/

Each presentation is from the USTP Technology Exposition that was held in May 2021 and June 2022.

Table 5-14: USTP Initiative GNC Projects

Project	University	Current Status	Reference
On-Orbit Demonstration of Surface Feature-Based Navigation and Timing	University of Texas, Austin	Still in development	USTP Technology Expo presentation
Autonomous Nanosatellite Swarming (ANS) using Radio Frequency and Optical Navigation	Stanford University	Onboard Starling mission (Launched in 2023)	USTP Technology Expo presentation
Distributed multi-GNSS Timing and Localization (DiGiTaL)	Stanford University	Leveraged technology used in Starling mission	USTP Technology Expo presentation
Mems Reaction Control and Maneuvering for Picosat beyond LEO	Purdue University	Awarded a suborbital flight test through NASA's Flight Opportunities program	(29)
A Small Satellite Lunar Communications and Navigation System	University of Boulder, Colorado	Still in development	USTP Technology Expo presentation

A high-precision continuous-time PNT compact module for the LunaNet small spacecraft	University of California, Los Angeles	Still in development	USTP Technology Expo presentation

5.3.1 Formation Flying and Rendezvous and Proximity Operations

Other GNC advances involve research on SmallSats performing precision formation flying (PFF) and on-orbit rendezvous and proximity operations (RPO). Many research papers have discussed ways to accomplish this, and previous extravehicular free flyers have demonstrated this innovative capability in the past few decades. To enable PFF and RPO missions, spacecraft require a suite of sensors to determine relative positions and attitudes to operate the navigation filters, complex guidance laws to maintain formations and prevent on orbit conjunctions, as well as advanced methods and/or actuators to control the relative states of the spacecraft. While some COTS sensors and actuators exist specifically for enabling PFF and RPO missions, current research and missions are using novel hardware and methods to achieve these objectives using existing components.

To enable relative guidance and control, it is important to first measure the relative positions and velocity, as well as attitude, of the spacecraft. Relative navigation can be accomplished by hardware specifically designed for the task, such as LiDAR, or repurposed hardware. For example, the PY4 mission has been able to demonstrate on-orbit range measurements between two spacecraft using their S-band radio modules with the addition of a GPS on the anchor spacecraft, and using a batch Kalman filter to determine the relative position vector of a target spacecraft to an accuracy of approximately 4 meters (34). The MR/MRS SAT mission seeks to use two vision-based cameras to perform stereo imaging to determine the relative position and velocity of an uncooperative space object without a priori knowledge to conduct its proximity operations (35). Another mission using vision-based systems was Seeker, a 3U CubeSat that was deployed in September 2019 and designed to demonstrate safe operations around a target spacecraft with core inspection capabilities. While Seeker was unable to perform its underlining goal, there were still several benefits for improving future missions (36). The CubeSat Proximity Operations Demonstration (CPOD) mission used an optics module with four imagers for relative ranging and target attitude determination but required priori knowledge and markers on the tracked spacecraft (37). More recently, the NASA Starling mission, launched in 2023, used an experimental onboard vision-based sensor payload called Starling Formation-flying Optical eXperiment (StarFOX) to provide angles-only relative navigation of an object without a priori knowledge, demonstrating on orbit relative position knowledge with only 0.5% error relative to range using one or multiple observers (38). These missions illustrate the complexity of the navigation problem, especially as much of it must be done autonomously without ground-based commanding to achieve the objectives of PFF and RPO missions.

Once the navigation solution is complete, guidance laws are used to determine path planning to achieve PFF and RPO objectives, as well as avoiding conjunction of objects when they are in near proximity. While this field is primarily research based and dependent on algorithms instead of COTS hardware, there is some development in packaged software suites to enable PFF and RPO type missions. The Autonomous Navigation, Guidance, and Control Software (autoNGC) suite is being developed by NASA Goddard Space Flight Center to enable autonomous operations when ground communications are limited or unavailable, a critical need for cis-lunar and deep space missions (39). Lockheed Martin, in collaboration with government and industry partners, is developing the 12U LINUSS platform that will eventually offer spacecraft upgrade and servicing capabilities, a service heavily dependent on PFF and RPO technologies (40). The

mission tested Lockheed Martin's Horizon Command & Control and Compass Mission Planning Software, which seeks to provide a software solution for various mission operations including PFF (41). It is expected that this field will grow with the continued increased interest in PFF and RPO missions and that demand for software suites with proven flight heritage will become more common.

While there have been multiple successful demonstrations of on-orbit relative navigation for missions conducting PFF and RPO objectives, many of these missions experienced difficulties with the control systems and their actuators. The Seeker mission experienced multiple failures with the thruster system likely related to a FPGA controller failure, resulting in the inability to thrust in multiple axes, causing the mission to not meet its minimum objective (36). CPOD is one of the more recent CubeSat missions to attempt the characterization of low-power proximity operations technologies, however it was only able to demonstrate limited RPO and was unable to complete the docking maneuvers as planned before its mission ended June 2023. The CPOD mission experienced partial solar panel failures resulting in lower power margins that limited mission operations, and experienced a propulsion system anomaly that was most likely related to a plenum leak. Even with these failures, the mission was able to demonstrate both far- and near-field rendezvous and ingress maneuvers, achieving most of the mission objectives. The spacecraft ran out of fuel completing some of these objectives, making it not possible to exercise the docking procedure which sought to use a magnetic actuator to dock the two spacecraft. The Lockheed Martin LINUSS mission also experienced a plenum leak and required continuous ground interventions by the development team to overcome the continual challenges experienced (40). The Starling swarm, which ended its initial mission in May 2024, experienced a leak in the propellant system and initially a sticky refill valve, though both anomalies were able to be resolved through ground operations (43). The mission was ultimately able to resume its in-train formation using thrusters to lower swarm member's altitude and let differential drag establish required separations, allowing the mission to continue conducting various experiments. Other missions had success using non-propulsive control techniques like drag separation for formation maintenance. The PY4 mission successfully used drag separation for both in-track and cross-track maneuvers by controlling individual member's attitude to create the requisite drag differential (44). While such missions are less prone to failure by not relying on a propulsion system, they are typically limited to far-field rendezvous and cannot achieve PFF or near-field RPO objectives like docking.

The complexity of PFF and RPO type missions for SmallSats continues to challenge the hardware, software, and operation design for these missions, however these challenges will continue to be overcome as more industry, government, and university entities become involved. With this field expanding, the benefits of PFF and RPO type missions will soon be realized for the SmallSat platform.

5.4 Summary

Conventional small spacecraft GNC technology is a mature area, with many high TRL components previously flown around Earth offered by several different vendors. These GNC techniques are generally semi/non-autonomous as on-board observations are collected with the assistance of ground-based intervention. As the interest for deep space exploration with small spacecraft grows, semi-to-fully autonomous navigation methods must advance. It is likely that future deep space navigation will rely solely on fully autonomous GNC methods that require zero ground-based intervention to collect/provide navigation data. This is a desirable capability as the spacecraft's dependence on Earth-based tracking resources (such as DSN) is reduced and the demand for navigation accuracy increases at large distances from Earth. However, current methods advancing deep space navigation involve both ground- and space-based tracking in

conjunction with optical navigation techniques. To support this maturity, the small spacecraft industry has seen a spike in position, navigation, and timing (PNT) technology progression in inertial sensors and atomic clocks, and magnetic navigation for near-Earth environments.

The rising popularity of SmallSats in general, and CubeSats in particular, means there is a high demand for components, and engineers are often faced with prohibitive prices. The Space Systems Design Studio at Cornell University is tackling this issue for GNC with their PAN nanosatellites. A paper by Choueiri et al. outlines an inexpensive and easy-to-assemble solution for keeping the ADCS system below $2,500 (45). Lowering the cost of components holds exciting implications for the future and will likely lead to a burgeoning of the SmallSat industry.

For feedback solicitation, please email: arc-sst-soa@mail.nasa.gov. Please include a business email so someone may contact you further.

References

(1) L.C.G Shepherd. and A.F.S.C Shepherd. “Space Surveillance Network.” Shared Space Situational Awareness Conference. Colorado Springs. 2006.

(2) D. Vallado, P. Crawford, R. Hujsak and T.S. Kelso. "Revisiting Spacetrack Report #3," AIAA 2006-6753. AIAA/AAS Astrodynamics Specialist Conference and Exhibit. August 2006.

(3) Thornton, C L and Border, J S: "Radiometric Tracking Techniques for Deep-Space Navigation." s.l: John Wiley & Sons, 2003.

(4) K. Kapás, T. Bozóki, G. Dálya et al. “Attitude determination for nano-satellites – I. Spherical projections for large field of view infrasensors.” Exp Astron 51, 515–527, 2021.

(5) JPL. “MarCO,” [Online] Available at: https://www.jpl.nasa.gov/missions/mars-cube-one-marco/

(6) J.R. Wertz. "Spacecraft attitude determination and control." Springer Science & Business Media. Vol. 73. 2012.

(7) AAC Clyde Space. IADCS200. [Online] Available at: https://www.aac-clyde.space/what-we-do/space-products-components/adcs/iadcs200

(8) AAC Clyde Space. IADCS400. [Online] Available at: https://www.aac-clyde.space/what-we-do/space-products-components/adcs/iadcs400

(9) Arcsec. Arcus ADCS. [Online] Available at: https://satsearch.co/products/arcsec-arcus-adcs

(10) Berlin Space Technologies. IADCS-100, datasheet. [Online] Available at: https://www.berlin-space-tech.com/portfolio/iadcs/

(11) Blue Canyon Technologies. Attitude Control Systems, datasheet. [Online] Available at: https://bluecanyontech.com/static/pdf/ACS.pdf

(12) CubeSpace Satellite Systems. CubeADCS. [Online] Available at: https://www.cubespace.co.za/products/cubeadcs/

(13) R. Kulczycki and P. Wisniewski. “Slew Maneuver Control for Spacecraft Equipped with Star Camera and Reaction Wheels.” 2005. Vol. 13, no. 3, pp. 349–356.

(14) J. L. Crassidis. "Spacecraft attitude determination." Encyclopedia of systems and control. 2021, Cham: Springer International Publishing. 2097-2104.

(15) B.B. Spratling and D. Mortari. ““A survey on star identification algorithms.” 2009.

(16) Jin, J, Ko, S and Ryoo, C K: “Fault Tolerant Control for Satellites with Four Reaction Wheels.” 2008. Vol. 16, no. 10, pp. 1250–1258.

(17) M.G. Finley, R.M. Broadfoot, S. Shekhar, and D.M. Miles. “Identification and removal of reaction wheel interference from in-situ magnetic field data using multichannel singular spectrum analysis.” 2023. Journal of Geophysical Research: Space Physics, 128, e2022JA031020. https://doi.org/10.1029/2022JA031020

(18) U. P. Sampaio, A. St-Amour, J. Lafontaine. “Zero-Speed Crossing Avoidance with Three Active Reaction Wheels using Set-Point Angular Momentum Management,.” 2016. IFAC-PapersOnLine, Volume 49, Issue 17. Pages 135-140, ISSN 2405-8963, https://doi.org/10.1016/j.ifacol.2016.09.024

(19) C.C. Liebe, "Star Trackers for Attitude Determination," IEEE Aerospace and Electronic Systems Magazine, vol. 10, no. 6, pp. 10-16, June 1995, doi: 10.1109/62.387971

(20) M.L. Psiaki, F. Martel, F and P.K. Pal. “Three-Axis Attitude Determination Via Kalman Filtering of Magnetometer Data.” Vol. 13, no. 3, pp. 506–514. 1990.

(21) J.H. Wessels. "Infrared Horizon Sensor for CubeSat Implementation." Master’s Thesis, Stellenbosch University. March 2018.

(22) A. Pelemeshko et al. "High-Precision CubeSat Sun Sensor Coupled with Infrared Earth Horizon Detector." 2020. IOP Conf. Ser.: Mater. Sci. Eng. Vol. 734. pp. 0121-8.

(23) M. M. Kobayashi et al. "The Iris Deep-Space Transponder for the SLS EM-1 Secondary Payloads." IEEE Aerospace and Electronic Systems Magazine, vol. 34, no. 9, pp. 34-44, 1 Sept. 2019.

(24) D. Greenheck et al. “Design and Testing of a Low-Cost MEMS IMU Cluster for SmallSat Applications.” 28th Annual AIAA/USU Conference on Small Satellites, 2014.

(25) S. Merhav. “Aerospace Sensor Systems and Applications.” Springer New York, 1998.

(26) O. Montenbruck et al. “Precision Spacecraft Navigation Using a Low-Cost GPS Receiver.” 2014. Vol. 16, no. 4, pp. 519–529.

(27) “Foreign Availability Determination Procedures and Criteria.” 2015. Office of the Federal Register. Title 15 Part 768.7.

(28) A. Hadhazy. "Cosmic GPS." Aerospace America. [Online] May 2020. Available at: https://aerospaceamerica.aiaa.org/features/cosmic-gps/

(29) J. Foust: "GPS in Space." MIT Technology Review. [Online] January 2002. https://www.technologyreview.com/2002/01/01/275613/gps-in-space/

(30) F.H. Aguirre. “X-Band Electronics for The INSPIRE CubeSat Deep Space Radio." 2015. IEEE Aerospace Conference.

(31) D. Baird. "NASA Tests Atomic Clock for Deep Space Navigation." [Online] 2018. Available at: https://www.jpl.nasa.gov/news/news.php?feature=7053

(32) J.W Kolar et al. "High-Speed Magnetically Levitated Reaction Wheels for Small Satellites." Anacapri, Capri: 23rd International Symposium on Power Electronics, Electrical Drives, Automation and Motion (SPEEDAM 2016), 2016.

(33) A.G. Cofer. "Film Evaporation Mems Thruster Array for Micropropulsion.” Open Access Dissertations. 1106. 2014. Available at: https://core.ac.uk/download/pdf/220145833.pdf

(34) M. Holliday, R. Ticknor, R. Hunter, J. Stupl, P. Fisch, I. Sow, J. Willis, and Z. Manchester. “The PY4 Mission: A Low-Cost Demonstration of CubeSat Formation-Flying Technologies.” 2024. Weekend Session VIII: Advanced Technologies - Research & Academia 2, 38th Annual AIAA/USU Small Satellite Conference, Logan UT.

(35) Jill Davis, Henry Pernicka. “Proximity operations about and identification of non-cooperative resident space objects using stereo imaging.” 2019. Acta Astronautica, Volume 155, Pages 418-425, ISSN 0094-5765, https://doi.org/10.1016/j.actaastro.2018.10.033.

(36) S. M. Pedrotty, “Seeker Overview and Mission 1 Review-- A New Development Approach for In-Space Inspectors.” 2021. [Online] Available at: https://www.nasa.gov/smallsat-institute/seeker-overview-and-mission-1-review--a-new-development-approach-for-in-space-inspectors

(37) J. Bowen, M. Villa, and A. Williams. “CubeSat based Rendezvous, Proximity Operations, and Docking in the CPOD Mission.” 2015. Weekend Session VIII: Advanced Technologies - Research & Academia 2, 29th Annual AIAA/USU Small Satellite Conference, Logan UT.

(38) J. Kruger, S. D’Amico, and S.S. Hwang. “Starling Formation-Flying Optical Experiment: Initial Operations and Flight Results.” 2024. Weekday Session 11: Advanced Technologies 2, 38th Annual AIAA/USU Small Satellite Conference, Logan UT.

(39) S. Hur-Diaz, B. Azimi, M. Romeo, A. Lionis, N. Stacey, R. Pritchett, G. Crum, and S. Semper. “Autonomous Navigation, Guidance, and Control Software in a Low SWaP Box.” 2024. Weekday Poster Session 5, 29th Annual AIAA/USU Small Satellite Conference, Logan UT.

(40) D. Barnhart, D. M. Shoemaker, E. T. King, T. Logue, and M. J. Lavis. “LM LINUSS™ - Lockheed Martin In-Space Upgrade Servicing System.” 2023. Weekday Session 9: Formation Flying and RPO, 37th Annual AIAA/USU Small Satellite Conference, Logan UT.

(41) Lockheed Martin. Horizon Command & Control (C2) and Compass Mission Planning Software. [Online] Available at: https://www.lockheedmartin.com/en-us/products/satellite-software.html

(42) I. A. Spiegal, B. Zhou, R. Goodloe, B. Fox, J. DiMatteo. “CubeSat Proximity Operations Demonstration (CPOD) Mission Results.” 2023. Weekday Session 9: Formation Flying and RPO, 37th Annual AIAA/USU Small Satellite Conference, Logan UT.

(43) T. Stevenson. “Flight Results and Lessons Learned From the Starling Propulsion System.” 2024. Weekday Session 7: Propulsion, 38th Annual AIAA/USU Small Satellite Conference, Logan UT.

(44) G. Falcone, J. B. Willis, Z. Manchester. “Propulsion-Free Cross-Track Control of a LEO Small-Satellite Constellation with Differential Drag.” 2023. Systems and Control, Electrical Engineering and Systems Science, Cornell University. Available at: https://arxiv.org/abs/2306.13844

(45) D. Dickinson. “NICER and SEXTANT demonstrate XNAV pulsar navigation system that may be used on Artemis.” 2020. [Online] Available at: https://skyandtelescope.org/astronomy-news/nasa-to-use-pulsar-navigation-for-deep-space-missions/